

Quantum detectors for the third cumulant of current fluctuations

Tero T. Heikkilä* and Teemu Ojanen

Low Temperature Laboratory, P.O. Box 3500, FIN-02015 TKK, Finland

(Dated: March 23, 2022)

We consider the measurement of the third cumulant of current fluctuations arising from a point contact, employing the transitions that they cause in a quantum detector connected to the contact. We detail two generic detectors: a quantum two-level system and a harmonic oscillator. In these systems, for an arbitrary relation between the voltage driving the point contact and the energy scales of the detectors, the results can be expressed in terms of an effective detector temperature T_{eff} . The third cumulant can be found from the dependence of T_{eff} on the sign of the driving voltage. We find that proper ordering of the fluctuation operators is relevant in the analysis of the transition rates. This is reflected in the effective Fano factor for the third cumulant measured in such setups: it depends on the ratio of the voltage and an energy scale describing the circuit where the fluctuations are produced.

I. INTRODUCTION

The statistics of current fluctuations in mesoscopic conductors have been at the center of interest within the last decade or so. This statistics can be described by the characteristic function, which is the Fourier transform of the probability density for a given value of the current. Characteristic functions for many different types of systems have been calculated, ranging from the simple case of a tunnel junction with Poisson distributed currents, to point contacts with binomial distribution and to more complicated systems composed for example of superconductors.^{1,2} Along with the characteristic function, the fluctuations can be described by the cumulants or moments of the distribution, the latter being of the form

$$M_n(t_1, \dots, t_n) = \langle \prod_{i=1, n} \delta I(t_i) \rangle, \quad (1)$$

where $\delta I(t_i) = I(t_i) - \langle I \rangle$, $I(t)$ is the instantaneous value of the current, and the brackets $\langle \cdot \rangle$ refer to ensemble averaging. Typically described observable is then the Fourier transform of $M_n(0, t_2 - t_1, \dots, t_n - t_1)$ with respect to the time differences $t_i - t_1$, and often only the limit where all the frequencies are taken to zero is known.

As many of the studied systems require quantum mechanics for their description, a natural question is the proper generalization of Eq. (1) to include the fact that the current operator $\hat{I}(t)$ may not commute with itself at different times. The answer to this question depends on how the fluctuations are to be measured. Levitov, Lee and Lesovik suggested the use of a spin coupled to the fluctuating current as an imaginary detector.³ More precisely, when the coupling is turned on at time $t = 0$, the angle of the spin coupled only to the fluctuating current $\hat{I}(t)$, with no average fields, starts to precess along with the current. Then the angle at a later time t , averaged

over the fluctuations, is

$$\sigma_+(t) = \sigma_+(0) \times \left\langle \tilde{T} \exp \left(i \frac{\tilde{g}}{2} \int_t^0 dt \hat{I}(t) \right) T \exp \left(-i \frac{\tilde{g}}{2} \int_0^t dt \hat{I}(t) \right) \right\rangle. \quad (2)$$

Here T and \tilde{T} denote the time- and anti-time-ordering operators and \tilde{g} is the coupling constant. This combination of time-ordering operators is also called the Keldysh ordering. For a classical current, ignoring noncommutativity, Eq. (2) would yield the characteristic function of the charge $Q = \int_0^t I(t)$ transmitted in a conductor in a given time t . Hence, Eq. (2) is one possible generalization of the characteristic function for a quantum current operator. In the language of quantum two-level systems (TLS's) or qubits, Eq. (2) describes the dephasing of a non-biased (zero level spacing) qubit.

The advantage of the spin detector is the fact that the Keldysh-symmetrized characteristic function of a point contact with transmission probability T_n for channel n is a product of binomial characteristic functions, described by the probability T_n of success. For example, the first three moments of the distribution of currents measured in that way are

$$\begin{aligned} \langle I \rangle &= G_0 V \sum_n T_n \\ \langle \delta I^2 \rangle &= G_0 e V \sum_n T_n (1 - T_n) \equiv F_2 e \langle I \rangle \\ \langle \delta I^3 \rangle &= G_0 e^2 V \sum_n T_n (1 - T_n) (1 - 2T_n) \equiv F_3 \langle I \rangle. \end{aligned}$$

Here $G_0 = e^2/h$ and the summation goes over the spin and the different transverse channels in the point contact. Such a characteristic function thus has a transparent classical interpretation.

But spin precession or qubit dephasing in real time is difficult to measure. Also, Levitov-Lee-Lesovik spin detector responds only to the zero-frequency noise. An alternative method is to measure the excitation and re-

laxation rates of a quantum system subject to a fluctuating force produced by the current. This is the approach taken in the present paper. These transition rates determine the static state of the density matrix for the system, which can in many cases be described by an effective temperature. Measuring the effective temperature is much more simple than spin precession, and it also gives access to the finite-frequency moments of the noise. In this paper we discuss how two simple quantum detectors behave in response to a non-Gaussian fluctuating force. An exact solution of this problem with the full characteristic function of fluctuations is not known to us, and therefore we resort to expanding in the cumulants of these fluctuations up to the third cumulant.

It turns out that in this case the proper way to define the third-order correlation function is by time-ordering two of the current fluctuation operators, and leaving the third one free (c.f., Eq. (3)).⁴ The relaxation of the qubit in this case is sensitive to the frequency dependence of the third cumulant,⁵ and the relevant Fano factor "measured" in this process depends on the relation between different frequency scales of the problem: If the qubit is "close" to the noise source, so that the frequency dependence is given by the voltage V applied over the scatterer, the third cumulant strength is characterized by $F_2 - F_3 = 2 \sum_n T_n^2 (1 - T_n) / \sum_n T_n$. This factor is very small for a tunnel junction, but finite for other types of scatterers. However, placing the qubit further from the noise source introduces another frequency scale into the problem, characterizing the circuit between the source and the qubit. For voltages above this frequency scale, the third cumulant effect on relaxation is characterized by the "usual" Fano factor, F_3 . In this limit one reproduces our results in Ref. 4, where we assumed that the frequency dependence is solely governed by the circuit. Besides the Fano factor, also the dependence on the voltage V is different in the two limits: in the first case it is logarithmic and in the second case linear.

Alternative "on-chip" detector schemes for measuring non-Gaussian fluctuations have been suggested in Refs. 6,7,8,9,10,11,12 and a few schemes have already been experimentally realized, see Refs. 13,14,15,16.

A. Frequency scales and different regimes

The noise source - detector system can be characterized with a few frequency/energy scales whose relative magnitudes determine the detector response. The main frequency scales are that coming from the detector level spacing Ω/\hbar , one characterizing the circuit connecting the noise source and the detector, say ω_c (for an example, see Ref. 4), and the rate Γ_{env} of transitions in the detector induced by its own environment. Furthermore, the fluctuations in a point contact are characterized by two further scales, given by the temperature T and the voltage V over the contact.

In this work, we assume that the level broadening is

sufficiently weak, i.e., $\hbar\Gamma_{\text{env}} \ll \Omega$, such that it can be taken into account perturbatively. The detector response will depend on the ratios between the voltage and the detector level spacing, eV/Ω (or, at a finite temperature, on $k_B T/\Omega$) and on the ratio $\hbar\omega_c/\Omega$. Finally, the response depends on the relative magnitude of the transition rates coming from the noise source and of those coming from the Gaussian bath.

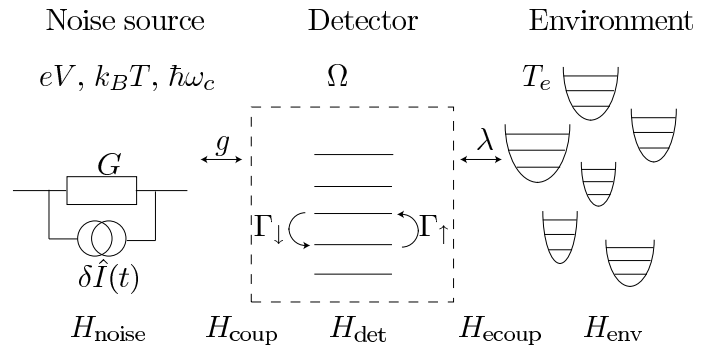


FIG. 1: Schematic idea of the fluctuation measurements: Current fluctuations in the noise source are coupled to a quantum detector, where they induce transitions between the detector energy levels. Another source for the transition rates is the intrinsic Gaussian environment of the detector, which can be modeled via an ensemble of harmonic oscillators. Up to the third order in the coupling coefficient g , the transition rates in the detector depend on the second and third cumulant of the fluctuations. As the latter is odd in the driving average current through the noise source, its effect can be measured by detecting the change in the rates when the sign of the driving average current is reversed.

II. EFFECT OF THIRD CUMULANT ON AN ARBITRARY DETECTOR

Consider the system depicted in Fig. 1. A non-Gaussian noise source is coupled to a detector whose state we aim to describe. The Hamiltonian of the system can be decoupled into

$$H = H_{\text{det}} + H_{\text{env}} + H_{\text{ecoup}} + H_{\text{noise}} + H_{\text{coup}}.$$

Here H_{det} is the Hamiltonian of the detector, specified in Secs. IV and V. It is in general described through a set of collective variables with mutually noncommuting operators \hat{A}_i . This detector is coupled to its own environment described by H_{env} through the coupling H_{ecoup} . We assume this environment to be Gaussian, such that we can model it via an ensemble of harmonic oscillators,¹⁷

$$H_{\text{env}} = \sum_j \hbar\omega_j \hat{a}_j^\dagger \hat{a}_j,$$

$$H_{\text{ecoup}} = \hat{A} \sum_j \lambda_j (\hat{a}_j^\dagger + \hat{a}_j) + \frac{1}{\hbar\omega_0} \hat{A}^2 \sum_j \lambda_j^2,$$

where $\hat{a}^{(\dagger)}$ is the bosonic annihilation (creation) operator of an oscillator in the bath, ω_n its eigenfrequency, and λ_j is the coupling constant from this oscillator to the system variable \hat{A} .

Finally, the noise source is described by H_{noise} and coupled to the detector via H_{coup} . The latter connects in general a set of collective variables of the noise source to another set of variables of the detector. As we aim to describe the measurement of current fluctuations, we explicitly assume that the previous is the current operator \hat{I} in the noise source.¹⁸ Thus the coupling is of the form

$$H_{\text{coup}} = \frac{\hbar}{e} \sum_i g_i \hat{I} \hat{A}_i,$$

where g_i are dimensionless coupling constants. We further assume that \hat{I} commutes with \hat{A}_i .

Including the effects of H_{coup} up to the third order in the coupling g_i , we do not have to specify H_{noise} , but it suffices to concentrate on the different correlators (cumulants) of \hat{I} . For simplicity, we include the effect of the average current on the detector Hamiltonian H_{det} , such that we can take $\langle \hat{I} \rangle = 0$. Here the brackets $\langle \cdot \rangle$ denote quantum averaging over the density matrix of the noise source. In particular, we concentrate on the noise power spectral density,

$$S_I(\omega) \equiv \int_{-\infty}^{\infty} dt e^{i\omega(t-t_0)} \langle \hat{I}(t) \hat{I}(t_0) \rangle,$$

and the partially time-ordered third cumulant^{4,19}

$$\begin{aligned} \delta^3 I(\omega_1, \omega_2) \equiv & \int_{-\infty}^{\infty} d(t_1 - t_0) d(t_2 - t_0) e^{i\omega_1(t_1 - t_0)} \\ & \times e^{i\omega_2(t_2 - t_0)} \langle \tilde{T}[\hat{I}(t_0) \hat{I}(t_1)] \hat{I}(t_2) \rangle. \end{aligned} \quad (3)$$

In a static system considered in this paper, these correlators are independent of the time t_0 .

Assume the uncoupled detector is described via the energy eigenstates $|n\rangle$ with energies E_n , i.e., $H_{\text{det}}|n\rangle = E_n|n\rangle$. Without coupling to the environment, the state of the detector is described by a density matrix $\rho_{nm}^{\text{det}}(t)$ which in general may show coherent oscillations between the different states. Assume now we turn on the couplings H_{coup} and H_{ecoup} at some time t_0 . If H_{coup} or H_{ecoup} do not commute with H_{det} , after some time $\rho_{nm}^{\text{det}}(t)$ tends into a diagonal steady state form.⁶ These diagonal entries $P_n \equiv \rho_{nn}^{\text{det}}(t \gg t_0)$ are obtained from a detailed-balance relation of the form

$$\frac{P_n}{P_m} = \frac{\Gamma_{m \rightarrow n}}{\Gamma_{n \rightarrow m}}. \quad (4)$$

In addition, the total probability has to be conserved, i.e., $\sum_n P_n = 1$. Here $\Gamma_{m \rightarrow n}$ is the total transition rate from the energy eigenstate m to the eigenstate n , due to the coupling to the environment.

Up to the third order in the coupling constants g_i and λ_i , the transition rates originating from the coupling to

the oscillator bath and the noise source are uncorrelated and we may write

$$\Gamma_{m \rightarrow n} = \Gamma_{m \rightarrow n}^{\text{env}} + \Gamma_{m \rightarrow n}^{\text{noise}}.$$

Here

$$\Gamma_{m \rightarrow n}^{\text{env}} = \frac{|A^{mn}|^2}{1 - e^{-\hbar\omega_{mn}/(kT_e)}} \sum_j \lambda_j^2 = e^{\hbar\omega_{mn}/(kT_e)} \Gamma_{n \rightarrow m}^{\text{env}}$$

is the transition rate from state m to state n due to the coupling of the detector to its Gaussian bath with temperature T_e , up to the second order in the coupling constants λ_j . Here $A^{mn} \equiv \langle m | \hat{A} | n \rangle$ and $\omega_{mn} \equiv (E_m - E_n)/\hbar$. In what follows, we use a short-hand notation $\lambda^2 \equiv \sum_j \lambda_j^2$. The transition rates induced by the noise source are of the form^{4,20}

$$\Gamma_{m \rightarrow n}^{\text{noise}} = \frac{1}{e^2} \sum_i g_i^2 |A_i^{mn}|^2 S_I(\omega_{mn}) + \Gamma_{m \rightarrow n}^{(3)}.$$

The rate from the third-order term is⁴

$$\Gamma_{m \rightarrow n}^{(3)} = \sum_i \frac{g_i^3}{e^3} \text{Re} \sum_l \left[\int d\omega \frac{\delta^3 I(\omega, -\omega_{mn})}{\omega - \omega_{ln} - i\eta} A_i^{ml} A_i^{ln} A_i^{nm} \right]. \quad (5)$$

Here η is a positive infinitesimal. In this paper, this integral is evaluated for two generic detectors in the case of noise originating from a point contact.

III. FREQUENCY DEPENDENT SECOND AND THIRD CUMULANTS OF A POINT CONTACT

A general scheme for calculating arbitrarily ordered frequency-dependent current correlators from the scattering theory was laid out by Salo, Hekking and Pekola (SHP) in Ref. 5. Their results are applied here in order to calculate the response of our generic detectors to the third-order current fluctuations. SHP decompose the operator describing the current through a given scatterer to "in" and "out" parts, $\hat{I} = \hat{I}_{\text{in}} - \hat{I}_{\text{out}}$, and show that time ordering between two current operators, $\hat{I}(t_1)$ and $\hat{I}(t_2)$, can be expressed in terms of ordering between \hat{I}_{in} and \hat{I}_{out} . For the latter, they find that a time-ordered product of a pair of (in,in) or (out,out) operators is the same as the unordered pair, and that time ordering a pair of (in,out) operators corresponds to an ordering where \hat{I}_{out} is placed to the left of \hat{I}_{in} .

A practically important noise source is a point contact with an energy independent scattering matrix. A "point contact" in this case refers to a system through which the electron time-of-flight τ_D is much smaller than the other time scales of the problem. In this case, the second-order correlator can be written in the form $S_I(\omega) = S_I^Q(\omega) + S_I^{\text{exc}}(\omega)$, where the vacuum fluctuations are $S_I^Q(\omega) = 2\hbar\omega G\theta(\omega)$, and the excess noise is given by^{7,21}

$$S_I^{\text{exc}}(\omega) = G\hbar\omega \left(\coth\left(\frac{\hbar\omega}{2kT}\right) - \text{sgn}(\omega) \right) + F_2 G \frac{eV \sinh(\frac{eV}{kT}) - 2\hbar\omega \coth(\frac{\hbar\omega}{2kT}) \sinh^2(\frac{eV}{2kT})}{\cosh(\frac{eV}{kT}) - \cosh(\frac{\hbar\omega}{kT})}$$

$$\xrightarrow{T \rightarrow 0} F_2 G (e|V| - \hbar|\omega|) \theta(e|V| - \hbar|\omega|).$$

Here G is the conductance of the point contact, V is the voltage applied over it, and $F_2 = [\sum_n T_n(1-T_n)]/\sum_n T_n$ is the Fano factor characterizing the transmission eigenvalues T_n of the contact. Written in this way, the excess noise is a symmetric function of frequency, and thus it contributes to excitation as much as to relaxation.

For the partially time-ordered third cumulant in the case of a point contact, one can deduce from the results of SHP²²

$$\delta^3 I(\omega_1, \omega_2) = S_{ioo}(-\omega_1 - \omega_2, -\omega_2) + S_{ioo}(\omega_1, -\omega_2) + S_{ioo}(-\omega_2, -\omega_1 - \omega_2) - S_{ooo}(-\omega_1 - \omega_2, -\omega_2). \quad (6)$$

Here

$$S_{ioo}(\omega_1, \omega_2) = eF_2 G [A(\omega_1, \omega_2 - v) - B(\omega_1, \omega_1 - \omega_2 - v)]$$

$$S_{ooo} = eF_3 G [A(\omega_1, \omega_2 - v) + A(\omega_1 - v, \omega_2) + A(\omega_1 + v, \omega_2 + v) - B(\omega_1, \omega_1 - \omega_2 - v) - B(\omega_1 - v, \omega_1 - \omega_2) - B(\omega_1 + v, \omega_1 - \omega_2 + v)],$$

$v = eV/\hbar$ and $F_3 = \sum_n T_n(1-T_n)(1-2T_n)/\sum_n T_n$. The functions $A(\omega_1)$ and $B(\omega_2)$ are defined as

$$A(x_1, x_2) \equiv \int dE f(E)(1-f(E+x_1))(1-f(E+x_2))$$

$$\xrightarrow{T \rightarrow 0} \theta(x_1)\theta(x_2) \min(x_1, x_2) \quad (7a)$$

$$B(x_1, x_2) \equiv \int dE f(E)(1-f(E+x_1))f(E+x_2)$$

$$\xrightarrow{T \rightarrow 0} \theta(x_1)\theta(x_1 - x_2) \min(x_1, x_1 - x_2), \quad (7b)$$

where $f(E)$ is a Fermi function.

In an electric circuit containing reactive elements, the fluctuation spectra are modified in a frequency dependent way. These types of modifications can be fairly generally calculated with a Langevin approach (see for example Refs. 23 and 24; for an exception relevant for the third cumulant, see Ref. 25). In the case of a time-independent average current, the noise spectra are modified according to

$$S_I^c(\omega) = G(\omega)G(-\omega)S_I^{\text{exc}}(\omega),$$

$$\delta^3 I^c(\omega_1, \omega_2) = G(\omega_1)G(\omega_2)G(-\omega_1 - \omega_2)\delta^3 I(\omega_1, \omega_2), \quad (8)$$

where $G(\omega)$ is a function characterizing the circuit. In what follows, we choose

$$G(\omega) = 1/(1 - i\omega/\omega_c), \quad (9)$$

typical for a circuit with reactive elements next to the point contact.

Below, we aim to calculate the outcome of these spectra on two generic detectors coupled to the noise source, a quantum two-level system and a harmonic oscillator.

IV. QUANTUM TWO-LEVEL SYSTEM

The general Hamiltonian for a quantum two-level system is

$$H_{TLS} = -\frac{\tilde{B}_z}{2}\sigma_z - \frac{B_x}{2}\sigma_x,$$

where $\sigma_{z/x}$ are Pauli matrices, and $B_{z/x}$ the effective magnetic fields. We assume that such a system is coupled to the noise source via a coupling Hamiltonian

$$H_{\text{coup}} = \frac{\hbar}{e}g(I + \delta\hat{I})\sigma_z.$$

The field pointing to the y -direction would not add any more generality to our model. The average current I can be included in the classical control field by defining $B_z \equiv \tilde{B}_z + 2\hbar gI/e$, so we can only concentrate on the fluctuations $\delta\hat{I}$.

The ground and excited states of this system are given by $|0\rangle = -\beta|\uparrow\rangle + \alpha|\downarrow\rangle$ and $|1\rangle = \alpha|\uparrow\rangle + \beta|\downarrow\rangle$, with $\alpha = \cos(\phi/2)$, $\beta = \sin(\phi/2)$ and $\phi = \arctan(B_z/B_x)$. The energies of these states are $E_{0/1} = \mp\Omega/2$, $\Omega \equiv \sqrt{B_x^2 + B_z^2}$.

Now, the second-order contribution to the excitation rates is

$$\Gamma_{0 \rightarrow 1}^{(2)} = \frac{g^2}{e^2} |\sigma_z^{01}|^2 S_{\text{noise}}(-\Omega/\hbar), \quad (10)$$

and the third-order contribution can be obtained from

$$\Gamma_{0 \rightarrow 1}^{(3)} = -\frac{g^3}{e^3} |\sigma_z^{01}|^2 \cos(\phi) \text{Re} \left[\int_{-\infty}^{\infty} d\omega \frac{\delta^3 I(\omega, \Omega/\hbar)}{\omega + \Omega/\hbar - i\eta} - \int_{-\infty}^{\infty} d\omega \frac{\delta^3 I(\omega, \Omega/\hbar)}{\omega - i\eta} \right]. \quad (11)$$

Here we used the fact that $\sigma_z^{11} = -\sigma_z^{00} = \cos(\phi)$. Note that the matrix element $|\sigma_z^{01}|^2 = \sin^2(\phi)$ is common for both rates. The corresponding relaxation rates $\Gamma_{1 \rightarrow 0}^{(2/3)}$ can be obtained from the excitation rates with the substitution $\Omega \rightarrow -\Omega$.

In the case of a point contact at a vanishing temperature ($k_B T \ll eV, \Omega$), the second-order excitation and relaxation rates are given by

$$\Gamma_{0 \rightarrow 1}^{(2)} = \frac{g^2}{e^2} |\sigma_z^{01}|^2 F_2 G \frac{(e|V| - \Omega) \theta(e|V| - \Omega)}{1 + (\Omega/\hbar\omega_c)^2} \quad (12a)$$

$$\Gamma_{1 \rightarrow 0}^{(2)} = \frac{g^2}{e^2} |\sigma_z^{01}|^2 G \left[\frac{F_2(e|V| - \Omega) \theta(e|V| - \Omega) + 2\Omega}{1 + (\Omega/\hbar\omega_c)^2} \right]. \quad (12b)$$

The calculation of the integrals required for the third-order effect in this case is detailed in Appendix A. The general result with an arbitrary ratio between eV and $\hbar\omega_c$ can be found analytically, but it is too long to be written down here. In the limit $\Omega < |eV| \ll \hbar\omega_c$ we obtain

$$\Gamma_{0 \rightarrow 1}^{(3)} = -\frac{g^3}{e^3} |\sigma_z^{01}|^2 \cos(\phi) [I_3 - I_1] = \frac{2g^3}{e^2} |\sigma_z^{01}|^2 \cos(\phi) G \text{sgn}(V) (F_2 - F_3) \left[\Omega \ln \left(\frac{|eV| - \Omega}{\Omega} \right) + |eV| \ln \left(\frac{|eV|}{|eV| - \Omega} \right) \right] \quad (13)$$

and $\Gamma_{1 \rightarrow 0}^{(3)} = -\Gamma_{0 \rightarrow 1}^{(3)}$. For $|eV| < \Omega$, the contributions to the excitation rates from the third cumulant vanish, but there is a contribution to the relaxation rate,

$$\Gamma_{1 \rightarrow 0}^{(3)} (|eV| < \Omega) = \frac{g^3}{e^2} |\sigma_z^{01}|^2 \cos(\phi) G F_2 \frac{8\pi \hbar^3 \omega_c^3 \Omega}{4\hbar^4 \omega_c^4 + 5\hbar^2 \omega_c^2 \Omega^2 + \Omega^4} V. \quad (14)$$

This contribution becomes small in the limit $\hbar\omega_c \gg \Omega$.

For $|eV| \gg \Omega$, these rates tend to $\pm \Gamma_{\text{close}}^{(3)}$ with

$$\Gamma_{\text{close}}^{(3)} = \frac{2g^3}{e^2} |\sigma_z^{01}|^2 \cos(\phi) G \text{sgn}(V) (F_2 - F_3) \Omega \left[\ln \left(\frac{|eV|}{\Omega} \right) + 1 - \frac{\Omega}{2|eV|} \right] + o \left(\left(\frac{\Omega}{|eV|} \right)^2 \right). \quad (15)$$

Note that for a tunnel junction, $F_2 = F_3$, and there is no contribution from the third cumulant to the transition rates. For other types of contacts, the rates are determined according to $F_2 - F_3 = 2 \sum_n T_n^2 (1 - T_n) / \sum_n T_n$. This is the same as the zero-frequency Fano factor one would get for an unordered third cumulant.⁵

In the opposite limit where the voltage by far exceeds the scale $\hbar\omega_c/e$ set by the circuit, the frequency dependence is governed by ω_c and the third-cumulant effect on the excitation rate is given by

$$\Gamma_{0 \rightarrow 1}^{(3)} = -\frac{4\pi g^3}{e^2} |\sigma_z^{01}|^2 \cos(\phi) F_3 \frac{G \hbar^3 \omega_c^3 \Omega}{4\hbar^4 \omega_c^4 + 5\hbar^2 \omega_c^2 \Omega^2 + \Omega^4} V \quad (16)$$

and again $\Gamma_{1 \rightarrow 0}^{(3)} = -\Gamma_{0 \rightarrow 1}^{(3)}$. This is the result one would obtain by assuming $\delta^3 I^c(\omega_1, \omega_2) \approx G(\omega_1) G(\omega_2) G(-\omega_1 - \omega_2) \delta^3 I(0, 0)$ as was done in Ref. 4.

The third-order contributions to the relaxation rates induced by the noise source are plotted in Fig. 2 for a few example cases.

Now let us analyze the detection of noise with the two-level system via the steady-state occupation probabilities P_0 and $P_1 = 1 - P_0$ of the states $|0\rangle$ and $|1\rangle$. These satisfy the detailed-balance condition, Eq. (4). Analogous to the equilibrium system, we can define an effective tempera-

ture of the quantum two-level system,

$$k_B T_{\text{TLS}} = \frac{\Omega}{\ln \left(\frac{P_0}{P_1} \right)} = \frac{\Omega}{\ln \left(\frac{\Gamma_{1 \rightarrow 0}^{(2)} + \Gamma_{1 \rightarrow 0}^{(3)}}{\Gamma_{0 \rightarrow 1}^{(2)} + \Gamma_{0 \rightarrow 1}^{(3)}} \right)} + o(g^4). \quad (17)$$

The contributions from the second and third cumulant can be separated by considering what happens to T_{TLS} when the voltage across the point contact is reversed. We define the average temperature $\bar{T}_{\text{TLS}} \equiv (T_{\text{TLS}}(V) + T_{\text{TLS}}(-V))/2$ and the difference $\Delta T_{\text{TLS}} \equiv T_{\text{TLS}} - T_{\text{TLS}}(-V)$. In the lowest order in the coupling constant g , the previous is then independent of the third cumulant, whereas the latter is directly proportional to it.

The limiting case expressions for \bar{T}_{TLS} and ΔT_{TLS} depend on the relative strengths of the relaxation/excitation rates from the bath and from the noise source, and on the magnitude of the circuit frequency scale ω_c . The previous is easiest to characterize through the ratio of the differences between relaxation and excitation they cause (this is essentially the "friction" strength in classical models),²⁹

$$\Lambda \equiv \lambda^2 \frac{e^2 (\hbar\omega_c^2 + \Omega^2) \sin^2(\phi)}{2\hbar^2 g^2 G \omega_c^2 \Omega}. \quad (18)$$

For $\Omega \ll k_B T_e, |eV|$, we then get an asymptotic expres-

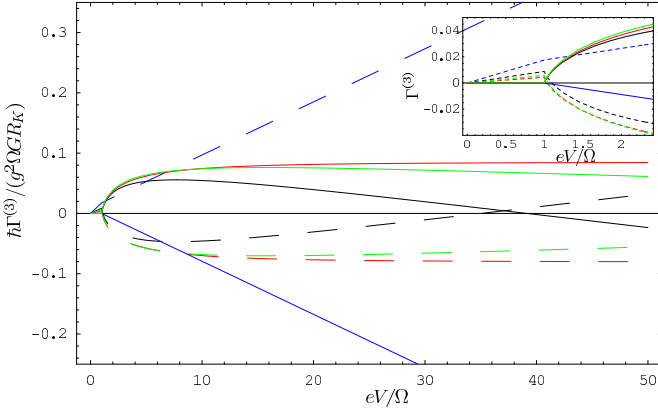


FIG. 2: (Color online): Third-order contributions to the excitation (solid lines) and relaxation (dashed lines) rates of a quantum two-level system coupled to a point contact. The rates are plotted for four different types of contacts with equal conductance G : tunnel contact (blue, $F_2 = F_3 = 1$), dirty interface²⁶ (black, $F_2 = 1/2$, $F_3 = 1/4$), diffusive wire²⁷ (red, $F_2 = 1/3$, $F_3 = 1/15$), and a chaotic cavity²⁸ (green, $F_2 = 1/4$, $F_3 = 0$). The other parameters used in this plot are $\phi = \pi/4$ and $\hbar\omega_c = 20\Omega$. Inset shows the low-voltage region. The rates are proportional to the dimensionless constant GR_K where $R_K = h/e^2$ is the resistance quantum.

sion for \bar{T}_{TLS} ,

$$k_B \bar{T}_{\text{TLS}} = \frac{2k_B T_e \Lambda + F_2 |eV|}{2(1 + \Lambda)} + \frac{(1 - F_2)\Omega}{2(1 + \Lambda)} + o\left(\frac{\Omega}{k_B T_e}\right). \quad (19)$$

For $|eV| \gg k_B T_e, \Omega$, there is another asymptotic expression,

$$k_B \bar{T}_{\text{TLS}} = \frac{F_2 |eV|}{2(1 + \Lambda)} + \frac{1 - F_2 + \Lambda \coth\left(\frac{\Omega}{2k_B T_e}\right)}{2(1 + \Lambda)} \Omega + o\left(\frac{\Omega}{|eV|}\right). \quad (20)$$

The latter equation is valid for an arbitrary ratio between Ω and kT_e .

The effective temperature T_{TLS} as a function of the voltage V is plotted in Fig. 3 for a few types of junctions and in Fig. 4 for a few values of ω_c .

The antisymmetric part ΔT_{TLS} of the temperature with respect to the voltage through the scatterer depends strongly on whether the frequency dependence is governed by the voltage or by the circuit. In the previous case, for $\Omega \ll k_B T_e, |eV| \ll \hbar\omega_c$ (noise source "close" to the detector), the asymptotic expression for ΔT_{TLS} is

$$k_B \Delta T_{\text{TLS}} = \text{sgn}(V) \frac{2g(F_2 - F_3) \cos(\phi)}{(1 + \Lambda)^2} \times (F_2 |eV| + 2k_B T_e \Lambda) \left[\ln\left(\frac{|eV|}{\Omega}\right) + 1 \right] + o\left(\frac{\Omega}{|eV|}\right). \quad (21)$$

For a noise source placed "far" from the detector, i.e.,

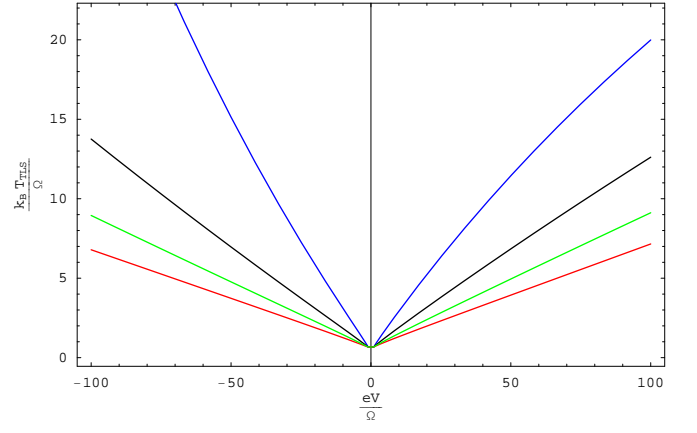


FIG. 3: Effective temperature of the two-level system as a function of the voltage through different types of point contacts coupled to it. The different curves correspond, from top to bottom, to a tunnel contact (blue), dirty interface (black), diffusive wire (green) and a chaotic cavity (red). The behavior is mostly dictated by the Fano factor F_2 . Other parameters in the plot are $g = 0.05$, $\hbar\omega_c = 20\Omega$, $\phi = \pi/4$, $\Lambda = 1$, $k_B T_e = \Omega$, and $G = 1/R_K$.

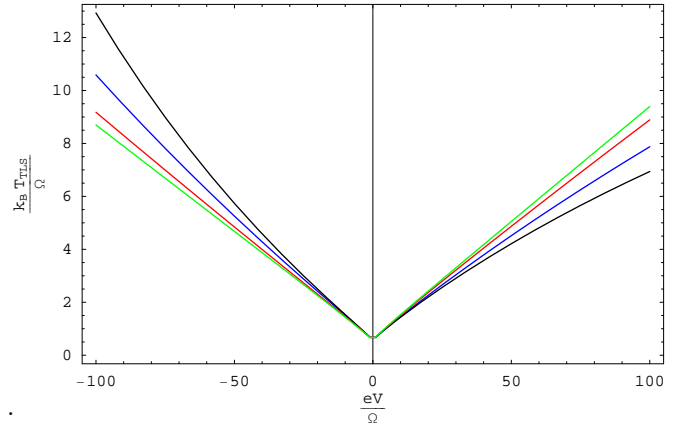


FIG. 4: Effective temperature of the two-level system as a function of the voltage through a diffusive point contact coupled to it via circuits characterized with different ω_c . In the right, from top to bottom: $\hbar\omega_c/\Omega = 100$ (green), 10 (red), 0.1 (blue) and 1 (black). Other parameters are as in Fig. 3.

$\Omega, \hbar\omega_c \ll |eV|, kT_e$, we get

$$k_B \Delta T_{\text{TLS}} = -V \cos(\phi) \frac{4gF_3\pi\hbar\omega_c}{(4\hbar^2\omega_c^2 + \Omega^2)(1 + \Lambda)^2} \times (F_2 |eV| + 2k_B T_e \Lambda) + o\left(\frac{\Omega, \hbar\omega_c}{|eV|}\right). \quad (22)$$

These limits are illustrated in Figs. 5 and 6 which show the temperature difference ΔT_{TLS} as a function of the voltage over the point contact for different types of point contacts and for different ω_c , respectively. For a tunnel junction, $\Delta T_{\text{TLS}}/V$ is negative for all values of the voltage as the logarithmic term in V (Eq. (21)) is absent, whereas for a chaotic cavity $F_3 = 0$ and the absence

of the linear term (Eq. (22)) leads to a positive definite $\Delta T_{\text{TLS}}/V$. For other types of junctions, there is a crossover from positive $\Delta T_{\text{TLS}}/V$ to a negative $\Delta T_{\text{TLS}}/V$ as eV roughly crosses $\hbar\omega_c$.

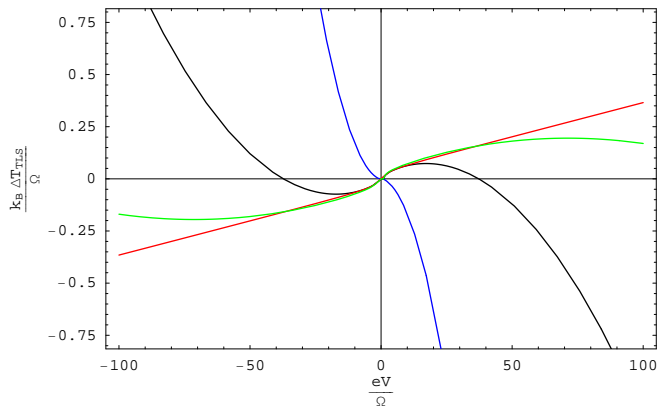


FIG. 5: Asymmetric part of the temperature ΔT_{TLS} as a function of the voltage over the point contact for different types of point contacts. In the right, from top to bottom: chaotic cavity (red), diffusive wire (green), dirty interface (black) and a tunnel junction (blue). Other parameters are as in Fig. 3.

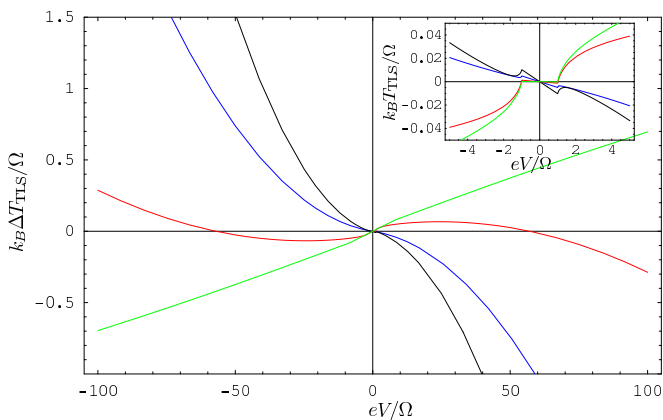


FIG. 6: Asymmetric part of the temperature ΔT_{TLS} as a function of the voltage over a diffusive point contact with different frequencies characterizing the circuit: in the right, from top to bottom: $\hbar\omega_c/\Omega = 100$ (green), 10 (red), 0.1 (blue), and 1 (black). Other parameters are as in Fig. 3. The curve for $\hbar\omega_c = 100\Omega$ is in the logarithmic regime, Eq. (21), for all plotted voltages, and it is characterized by the Fano factor $F_2 - F_3$. The curves for $\hbar\omega_c \leq 1$ are in the linear regime, Eq. (22), and the case $\hbar\omega_c = 10\Omega$ has a crossover between the two. Inset shows the low-voltage regime, reflecting the behavior described in Eq. (14).

The relative temperature change $\Delta T_{\text{TLS}}/\bar{T}_{\text{TLS}}$ is thus logarithmic in V for $\Omega, k_B T_e \ll |eV| \ll \hbar\omega_c$ and linear for $|eV| \gg \Omega, k_B T_e, \hbar\omega_c$.

V. HARMONIC OSCILLATOR

Below, we discuss two schemes for using a quantum harmonic oscillator as a detector of the current fluctuations. The first scheme couples a displaced oscillator to the fluctuations through the position operator \hat{x} , and the second scheme through the second power of the momentum operator, \hat{p}^2 . It turns out that at least up to the third order in the coupling operators g_i, λ_i , the first scheme is insensitive to the third cumulant, whereas the latter follows quite closely the qubit scheme. First, we note that a simple harmonic oscillator coupled to the fluctuations via its position operator, i.e., $\hat{A} = \hat{x}$ directly implies $\Gamma^{(3)} = 0$ as Eq. (5) requires that all the matrix elements between the initial, the final, and one or more intermediate states are nonzero. This cannot be satisfied as \hat{x} couples only the neighboring states.

A. Displaced harmonic oscillator coupled to the position operator

This restriction may be overcome by considering a *displaced* harmonic oscillator, so that the effective coupling is to $\hat{x} - x_0$, where x_0 is a scalar displacement. However, one can quite generally show that even in this case the resulting $\Gamma^{(3)} = 0$.

To be specific, consider a harmonic oscillator coupled to the fluctuating current. The Hamiltonian for the oscillator is

$$H_{\text{HO}} = -\frac{\hbar}{2m} \partial_x^2 + \frac{1}{2} m \omega_0^2 \hat{x}'^2.$$

Assume the fluctuating current is coupled to the \hat{x}' -coordinate, i.e., the coupling is described by

$$H_{\text{coup}} = \frac{g}{e} (I_b + \delta \hat{I}) \sqrt{2m\hbar\omega_0} \hat{x}'.$$

Due to the average current term I_b , the oscillator potential minimum is shifted from $x = 0$ to $x_0 = -\sqrt{2\hbar g I_b} / (e\sqrt{m\omega_0^3})$. Defining a new displaced operator $\hat{x} \equiv \hat{x}' - x_0$ we get, neglecting the unimportant scalar terms,

$$H_{\text{HO}} + H_{\text{coup}} = -\frac{\hbar}{2m} \partial_x^2 + \frac{1}{2} m \omega_0^2 \hat{x}^2 + g \frac{\sqrt{2m\omega_0}}{e} \delta \hat{I} (\hat{x} + x_0). \quad (23)$$

In what follows, we assume that I_b can be controlled separately from the current flowing through the noise source. This type of a separation of average and noise currents was discussed for example in Ref. 30.

We proceed in the usual way by defining the harmonic oscillator annihilation and creation operators,

$$\begin{cases} \hat{a} \\ \hat{a}^\dagger \end{cases} = \frac{1}{\sqrt{2\hbar m \omega_0}} (m\omega_0 \hat{x} \mp \hbar \partial_x).$$

Now the energy eigenstates $|n\rangle$ of the "average" Hamiltonian are those of the number operator, $\hat{N}|n\rangle = \hat{a}^\dagger \hat{a}|n\rangle = |n\rangle$. The fluctuations are coupled to the operator $\hat{A} \equiv \sqrt{2m\hbar\omega_0}(\hat{x} + x_0)$. This has a finite matrix element $A_{n,n\pm 1}$ between the neighboring states due to the operator \hat{x} . Moreover, the displacement x_0 makes the diagonal matrix element \hat{A}_{nn} also finite, and independent of the level index n . Similar to the two-level system, we can write the second-order excitation and relaxation rates due to the external noise from a point contact at $k_B T \ll |eV|, \hbar\omega_0$,

$$\Gamma_{n \rightarrow n+1}^{(2)} = \frac{g^2}{e^2} (n+1) S_I(-\omega_0) \quad (24a)$$

$$= \frac{g^2}{e^2} (n+1) G F_2(|eV| - \hbar\omega_0) \theta(|eV| - \hbar\omega_0)$$

$$\Gamma_{n+1 \rightarrow n}^{(2)} = \frac{g^2}{e^2} (n+1) S_I(\omega_0) \quad (24b)$$

$$= \frac{g^2}{e^2} (n+1) G [F_2(|eV| - \hbar\omega_0) \theta(|eV| - \hbar\omega_0) + 2\hbar\omega_0].$$

The third-order contribution to the excitation rate is

$$\Gamma_{n \rightarrow n+1}^{(3)} = \frac{2g^4 I_b}{e^4 \omega_0} (n+1) \text{Re} \left[\int_{-\infty}^{\infty} d\omega \frac{\delta^3 I(\omega, \Omega/\hbar)}{\omega + \Omega/\hbar - i\eta} + \int_{-\infty}^{\infty} d\omega \frac{\delta^3 I(\omega, \Omega/\hbar)}{\omega - i\eta} \right] \quad (25)$$

and the relaxation rate $\Gamma_{n+1 \rightarrow n}^{(3)}$ can be obtained by replacing ω_0 by $-\omega_0$ inside the integrals (but not in the prefactor).

These integrals are the same as for the quantum two-level system, Eq. (11), up to a sign between them. But as shown in Appendix A, the two integrals give exactly the opposite contribution under quite general conditions, and therefore $\Gamma^{(3)}$ vanishes.

B. Coupling to the square of the momentum or position operator

Assume one could vary the mass of the harmonic oscillator via the fluctuating current. In this case, the coupling to the fluctuations would be of the form³¹

$$H_{\text{coup}} = \frac{\delta \hat{m}(\delta \hat{I})}{2m^2} \hat{p}^2 = -g \delta \hat{I} (\hat{a}^\dagger - \hat{a})^2. \quad (26)$$

Such an operator $\hat{A} = (\hat{a}^\dagger - \hat{a})^2$ has finite matrix elements between next-nearest neighbor energy levels n and $n+2$ of the oscillator, $A_{n,n+2} = \sqrt{(n+1)(n+2)}$ and diagonal matrix elements, $A_{n,n} = -2n - 1$. To be able to further describe the system with an effective temperature, we assume that the coupling to the bath is much weaker than the coupling to the noise source, and the previous can hence be neglected. Now the second-order contribution

to the transition rates due to the current fluctuations at $T = 0$ are

$$\Gamma_{n \rightarrow n+2}^{(2)} = \frac{g^2}{e^2} (n+1)(n+2) S_I(-2\omega_0) \quad (27a)$$

$$= \frac{g^2}{e^2} (n+1)(n+2) G F_2(|eV| - 2\hbar\omega_0) \theta(|eV| - 2\hbar\omega_0)$$

$$\Gamma_{n+2 \rightarrow n}^{(2)} = \frac{g^2}{e^2} (n+1)(n+2) S_I(2\omega_0) \quad (27b)$$

$$= \frac{g^2}{e^2} (n+1)(n+2) G [F_2(|eV| - 2\hbar\omega_0) \theta(|eV| - 2\hbar\omega_0) + 4\hbar\omega_0].$$

The third-order contribution to the excitation rate is

$$\Gamma_{n \rightarrow n+2}^{(3)} = -\frac{g^3}{e^3} (n+1)(n+2) \text{Re} \left[(2n+1) \times \int_{-\infty}^{\infty} d\omega \frac{\delta^3 I(\omega, 2\omega_0/\hbar)}{\omega + 2\omega_0 - i\eta} + (2n+3) \int_{-\infty}^{\infty} d\omega \frac{\delta^3 I(\omega, 2\omega_0/\hbar)}{\omega - i\eta} \right] \quad (28)$$

$$\equiv -\frac{g^3}{e^3} (n+1)(n+2) [(2n+1)I_3 + (2n+3)I_1]$$

and the relaxation rate $\Gamma_{n+2 \rightarrow n}^{(3)}$ can be obtained by replacing ω_0 by $-\omega_0$. Using the fact that $I_3 = -I_1$ (see Appendix A), we get

$$\Gamma_{n \rightarrow n+2}^{(3)} = -\frac{2g^3}{e^3} (n+1)(n+2) I_1(2\omega_0). \quad (28)$$

The third-order rate has thus the same level-dependent prefactor as the second-order rate. Therefore, we can again define an effective temperature, which now is of the form

$$k_B T_{\text{ho}} = \frac{2\hbar\omega_0}{\ln \left(\frac{\Gamma_{n+2 \rightarrow n}^{(2)} + \Gamma_{n+2 \rightarrow n}^{(3)}}{\Gamma_{n \rightarrow n+2}^{(2)} + \Gamma_{n \rightarrow n+2}^{(3)}} \right)}. \quad (29)$$

This is independent of the level index n , provided the fluctuations coupling linearly to \hat{x} or \hat{p} can be neglected.

Because of the similar form of the rate expressions as in the qubit case, the behavior of the effective temperature is similar to the qubit, provided the prefactor $\cos(\phi)$ in Eqs. (15,16,21,22) is replaced by -1 and the matrix element σ_z^{01} by $(n+1)(n+2)$. In the case of coupling to \hat{x}^2 instead of \hat{p}^2 (i.e., varying the spring constant rather than the mass), the only difference is the inverted sign of the third-cumulant contributions to the rates.

VI. EXPERIMENTAL DETECTOR REALIZATIONS

To exemplify the measurement of the third cumulant through the polarization of a qubit coupled to the fluctuating current, we consider three specific examples: a persistent current (or a flux) qubit,^{32,33} a phase

qubit,^{34,35} and a charge qubit.³⁶ The fluctuation measurement schemes with these qubits are illustrated in Fig. 7. Apart from the measurement schemes, we aim to discuss typical values for the coupling constant g , level splitting Ω , circuit frequency scale ω_c , and the dimensionless constant Λ characterizing the ratio between the intrinsic and induced noise.

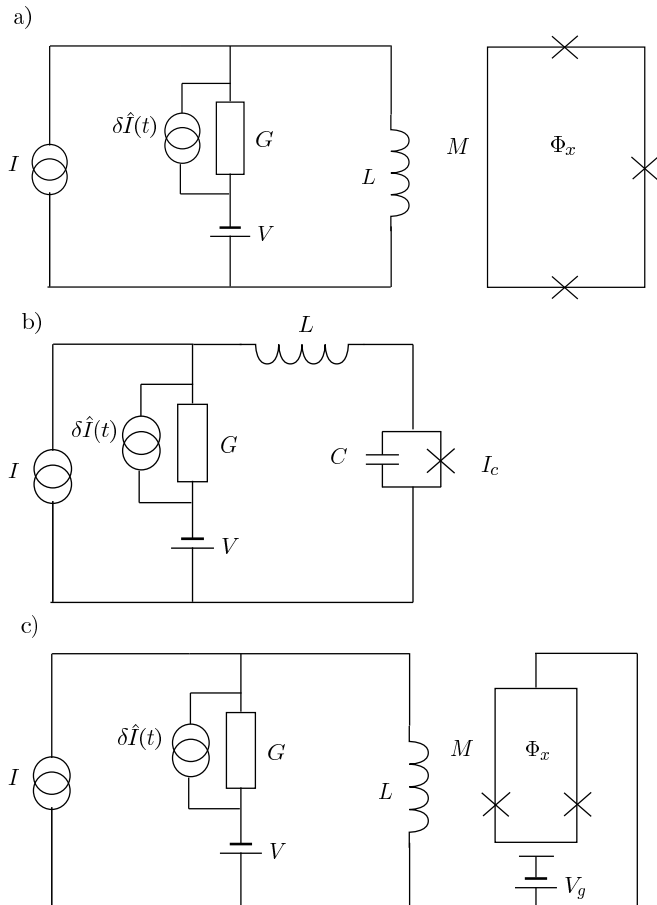


FIG. 7: Fluctuation measurement schemes using superconducting qubits: a) Persistent current qubit, b) phase qubit, and c) charge qubit.

In all cases, the level splitting Ω/\hbar turns out to be of the order of a few GHz at minimum. Also, for all systems the relevant reactive element causing dispersion of noise is the inductance L of the lines feeding the noise current, and therefore the frequency scale $\omega_c = 1/(GL)$, where G is the conductance of the shot noise source. As L is typically of the order of some 10 pH, and R may vary between some 10 Ω to some 100 k Ω , we have ω_c ranging between 10^3 to 10^6 GHz. This means that unless special care is taken to make a large inductance, $\hbar\omega_c/\Omega$ is at least a few hundred.

However, note that at least in diffusive wires and chaotic cavities, there is an additional frequency scale given by the inverse dwell time $1/\tau_D$ or the inverse screening time $1/\tau_{sc}$.^{37,38,39} For example, for a diffusive wire of length $L = 1\mu\text{m}$ and diffusion constant $D = 100\text{ cm}^2/\text{s}$,

we have $1/\tau_D \approx 10\text{ GHz}$. When $1/\tau_D$ or $1/\tau_{sc}$ is less than $\min(|eV|/\hbar, \omega_c)$, these have to be taken into account separately.

With the qubits, the detection takes place by applying a steady current through the noise source, and measuring the occupation number ρ_{11} of the higher qubit state many times, i.e., averaging over the realizations of current fluctuations. The effective temperature is then

$$k_B T_{\text{eff}} = \Omega \ln \left(\frac{1 - \rho_{11}}{\rho_{11}} \right).$$

The third-cumulant effect can be controlled by tuning the phase ϕ through the average fields B_x and B_z . When either of these fields vanishes, also the third-cumulant effect should vanish.

The temperature measurement of the harmonic oscillator depends on its realization: For a true oscillator based on a resonant LC -circuit, the temperature should be measured either by measuring the current noise power in the oscillator, or coupling it to a nonlinear system, say a SQUID, and measuring its response. If the realization is a current-biased Josephson junction, the temperature detection can be done via the measurement of the thermal escape rate as in Ref. 30.

Voltage fluctuations could also be coupled to the qubits or oscillators. Typically these would couple to the perpendicular external field component compared to the current fluctuations. However, the frequency dependence of the third cumulant of voltage fluctuations is not known, and the response of the qubits might in this case be somewhat different.

A. Persistent current qubit

In the persistent current qubit, a fluctuating current is easiest to couple to the qubit current through the mutual inductance M as in Fig. 7a.³² In the basis defined by the clockwise and anticlockwise current, this corresponds to coupling to σ_z . In this case, the coupling constant g is of the order of

$$g_{pcq} = \frac{e}{\hbar} M \Delta I_{qb} \sim \frac{e}{\hbar} M I_c,$$

where ΔI_{qb} is the different between the currents corresponding to the two qubit states. This is of the order of the critical current I_c of the Josephson junctions. Using $M \approx 2\text{ pH}$ and $I_c \approx 3\text{ }\mu\text{A}$ close to the experimental values,^{32,33} we get $g \approx 0.01$. Finally, with the intrinsic relaxation time $T_1 = 1\text{ ms}$, $\Omega/\hbar = 10\text{ GHz}$, $R = R_K$ and $\phi = 0$, we get $\Lambda \approx 0.003$, i.e., the intrinsic bath effect is almost negligible.

B. Phase qubit

With the scheme depicted in Fig. 7b, the external current fluctuations can be again coupled to the diagonal

element of the qubit Hamiltonian, i.e., σ_z . The coupling strength is³⁴

$$g_{pq} = \frac{e}{\hbar} \frac{\partial E_{10}}{\partial I_b},$$

where E_{10} is the level separation between the qubit states. For the bias current close to I_c , this is given by

$$E_{10} \approx \hbar\omega_p(I) \left(1 - \frac{5}{36} \frac{\hbar\omega_p(I)}{\Delta U(I)} \right),$$

where $\omega_p(I) = 2^{1/4} \sqrt{8E_J E_C} (1 - I/I_c)^{1/4}$ and $\Delta U(I) = 4\sqrt{2}/3 E_J (1 - I/I_c)^{3/2}$, $E_J = \hbar I_c / (2e)$ and $E_C = e^2 / (2C)$ are the Josephson and charging energies of the junction, and I_c is its critical current. Thus we have

$$g_{pq} = - \frac{5\tilde{e}_C + 3 \cdot 2^{3/4} \sqrt{\tilde{e}_C} (1 - i_b)^{5/4}}{6(1 - i_b)^2}$$

where $i_b = I/I_c$, and $\tilde{e}_c = E_C/E_J$. With the values³⁵ $C = 6$ pF and $I_c = 21$ μ A and $i_b \approx 0.99$, we get $g_{pq} \approx 0.1$. In such qubits, the relaxation due to the intrinsic bath is slower than $\omega_p/1000$, which implies $\Lambda < 0.1$. Therefore, the intrinsic bath should also here be negligible.

C. Charge qubit

Coupling a charge qubit in a form of the Cooper pair box³⁶ to current fluctuations takes place via the operator σ_x in the natural charge basis of the qubit. This is accomplished by coupling the fluctuations to the flux controlling the Josephson energy of the Cooper pair box. Due to this slightly different type of a coupling, the phase ϕ should be defined as $\phi = \arctan(B_x/B_z)$, but otherwise the rate expressions stay the same. In this case, the coupling strength is given by⁴⁰

$$g = \frac{e}{\hbar} M \frac{dI_c(\Phi_x)}{d\Phi_x},$$

where M is the mutual inductance and $I_c(\Phi_x)$ is the critical current of the box at the average external flux Φ_x . With $M = 2$ pH and $I_c = 300$ nA, g can be made to vary between almost zero (the "sweet spot" where the first derivative of $I_c(\Phi_x)$ vs. Φ_x vanishes) to some 10^{-3} . A higher coupling strength can be obtained by increasing I_c and thereby going away from the strict charge basis as in Ref. 41.

D. Cooper pair box in a resonant circuit

Coupling the fluctuations to a flux controlling the Josephson coupling of a Cooper pair box placed in a resonant circuit, one may control the effective capacitance of the resonator.^{42,43,44} Such a setup corresponds to that studied in Subs. V B. The coupling strength g depends

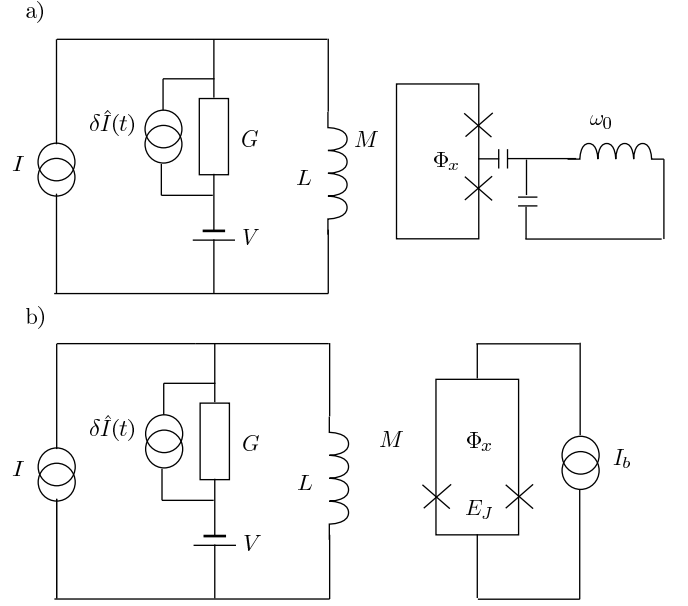


FIG. 8: Fluctuation measurements with oscillators whose mass or spring constant is driven with the fluctuations: a) Cooper-pair box and b) driven Josephson junction. In both cases, the Josephson energy is tuned with the fluctuations. In a), the difference to a charge qubit is in the fact that the transistor is placed as a part of a resonant circuit.

on the relative ratio between the Josephson and charging energies, E_J and E_C of the Cooper pair box. For $E_J = 10E_C$, the relative capacitance modulation $\Delta C/C$ can be of the order of 0.05 for a change $\Delta\Phi_x = \hbar/2e$ in the external flux.⁴³ The coupling constant in this case is

$$g = - \frac{\Delta C}{C} \frac{e^2 M \omega_0}{2\hbar}.$$

For $M = 100$ pH and $\omega_0 = 100$ GHz, we would hence obtain $g \sim 10^{-4}$. This is quite a small value, and using this scheme would require optimization of the E_J/E_C -ratio and maximizing both M and ω_0 .

E. Current biased SQUID

Instead of directly controlling the bias current of the Josephson junction as in the phase qubit scheme above, one may also envisage coupling the fluctuations inductively to control the flux in a SQUID as in Fig. 8b. The Hamiltonian of a biased symmetric SQUID is

$$H_{JJ} = -4E_C \partial_\varphi^2 - E_J \cos \left(2\pi \frac{\Phi_x}{\Phi_0} \right) \cos(\varphi) - \frac{\hbar}{2e} I_b \varphi,$$

where φ is the phase across the SQUID, I_b is the bias current, Φ_x is the external flux through the loop, and $\Phi_0 = h/(2e)$ is the flux quantum. We assume the self-inductance of the loop small enough, so that it can be neglected. For I_b much lower than the critical current

$I_C(\Phi_x) = 2e/\hbar E_J \cos(2\pi\Phi_x/\Phi_0)$ of the SQUID, and E_C , $k_B T_{JJ} \ll E_J$, we can neglect the driving term and expand the term $\cos(\varphi) \approx 1 - \varphi^2/2$. As a result, we get a harmonic oscillator Hamiltonian with the mass given by the capacitance C , and the spring constant given by the Josephson inductance $L_J = \hbar/(2e)I_C$. Now connecting the current fluctuations to the flux $\Phi_x = M(I + \delta I(t))$, we can vary the inductance term, i.e., couple to \hat{x}^2 of the harmonic oscillator. The coupling constant is given by⁴⁵

$$g_{JJ} = -\frac{M e^2 \omega_p}{2\hbar} \sin\left(2\pi \frac{MI}{\Phi_0}\right),$$

where $\omega_p = \sqrt{8E_J E_C/\hbar}$ is the plasma frequency of the SQUID at $\Phi_x = 0$. With $M = 20$ pH, $\omega_p = 200$ GHz, we get $g = 10^{-3}$. Hence, the current biased SQUID can be used for the detection of the third cumulant in the harmonic mode, but the parameters M and ω_p need to be optimized to quite high values in order to obtain large enough coupling strength.

Another way to use the SQUID in the harmonic mode would be to place it in a resonant circuit, and use the modulation of the Josephson inductance for the fluctuation measurement. In this case, the scheme would be similar to that presented in Subs. VID, but the coupling would be to \hat{x}^2 rather than \hat{p}^2 . The coupling constant would be again given by Eq. (VIE), but now ω_p should be replaced with the resonance frequency of the circuit.

VII. DISCUSSION

We suggest to use the excitation and relaxation in quantum two-level systems or harmonic oscillators for

measuring the third cumulant of current fluctuations in a short contact. When coupled to the driven non-Gaussian fluctuations, the static density matrix of these systems reveals information on the frequency dependence of these fluctuations. The third cumulant can be read from the change in the effective temperature of these systems upon reversing the polarity of the bias across the contact. As the measured signal is inherently quantum, the ordering of the current operators turns out to be important. Depending on the relative ratio of the frequency scales of the system, given by the voltage, eV/\hbar , and the circuit, ω_c , the measured Fano factor for the third cumulant is either $\sum_n T_n(1 - T_n)(1 - 2T_n)/\sum_n T_n$ ($eV \gg \hbar\omega_c$, Eqs. (13) and (21)) or $2\sum_n T_n^2(1 - T_n)/\sum_n T_n$ ($eV \ll \hbar\omega_c$, Eqs. (16) and (22)). This slightly resembles the reasoning in Ref. 46, where the measured Fano factor depends on "how far" the detector is placed from the current path.

Acknowledgements

We thank Joachim Ankerhold, Pertti Hakonen, Matthias Meschke, Jukka Pekola and Peter Samuelsson for enlightening discussions. This work was supported by the Academy of Finland.

APPENDIX A: INTEGRALS REQUIRED FOR THE THIRD-ORDER RATES

The third-order contributions to the rates depend on the integrals of the form

$$I_{1/4} \equiv \text{Re} \left[\int_{-\infty}^{\infty} \frac{\delta^3 I(\omega, \pm\omega_0)}{\omega} d\omega \right] = \text{Re} \left[\int_0^{\infty} \frac{\delta^3 I(\omega, \pm\omega_0) - \delta^3 I(-\omega, \pm\omega_0)}{\omega} d\omega \right]$$

$$I_{2/3} \equiv \text{Re} \left[\int_{-\infty}^{\infty} \frac{\delta^3 I(\omega, \mp\omega_0)}{\omega \mp \omega_0} d\omega \right] = \text{Re} \left[\int_0^{\infty} \frac{\delta^3 I(\omega \mp \omega_0, \mp\omega_0) - \delta^3 I(-\omega \mp \omega_0, \mp\omega_0)}{\omega} d\omega \right].$$

Quite generally, the frequency dependent third cumulant considered in this manuscript satisfies $\delta^3 I(\omega_1, \omega_2) = \delta^3 I(-\omega_1 - \omega_2, \omega_2)$. This is valid for a point contact at arbitrary temperature (Eqs. (6) – (7)) in the presence ($\delta^3 I^c$ from Eq. (8)) or absence of the external circuit. Using this symmetry, it is straightforward to show that $I_2 = -I_4$ and $I_3 = -I_1$.

The integrals can be calculated at $T = 0$ by evaluating $(\delta^3 I(\omega, \pm\omega_0) - \delta^3 I(-\omega, \pm\omega_0))/\omega$ by parts, $\omega \in [0, \min(\omega_0, |eV|/\hbar - \omega_0)]$, $\omega \in [\min(\omega_0, |eV|/\hbar - \omega_0), \max(\omega_0, |eV|/\hbar - \omega_0)]$, $\omega \in [\max(\omega_0, |eV|/\hbar - \omega_0), |eV|/\hbar]$ and finally $\omega > |eV|/\hbar$. In the presence

of the external circuit, described with Eq. (9), the resulting analytic expressions for I_i are very long, even at zero temperature. However, they have rather simple limits depending on the relation between $|eV|$ and $\hbar\omega_0$, i.e., which of these scales gives the cutoff for the integrals. For all $\hbar\omega_c$, the integrals are finite only for $|eV| > \Omega$. Moreover, in both limits (but not generally), $I_1 = I_2$.

For $|eV| \ll \hbar\omega_c$ we get for $T = 0$

$$I_1 = eG(F_2 - F_3)\text{sgn}(V) \left[\Omega \ln \left(\frac{|eV| - \hbar\omega_0}{\omega_0} \right) + |eV| \ln \left(\frac{|eV|}{|eV| - \hbar\omega_0} \right) \right]. \quad (\text{A1})$$

For $|eV| \gg \hbar\omega_c$, the integral can be evaluated by assuming a frequency independent intrinsic third cumu-

lant, $\delta^3 I(\omega_1, \omega_2) = G(\omega_1)G(\omega_2)G(-\omega_1 - \omega_2)F_3 eGV$ as was done in Ref. 4. This yields

$$I_1 = -eGF_3 \frac{2\pi\omega_c^3\omega_0}{4\omega_c^4 + 5\omega_c^2\omega_0 + \omega_0^2}. \quad (\text{A2})$$

This result can be found fairly straightforwardly via the residue theorem.

-
- * Correspondence to Tero.Heikkila@tkk.fi
- ¹ Y. Nazarov, ed., *Quantum Noise in Mesoscopic Physics*, vol. 97 of *Nato Science Series II* (Kluwer, Dordrecht, 2003).
 - ² W. Belzig, in *Proceedings of Summer School/Conference on Functional Nanostructures* (2003), [cond-mat/0312180].
 - ³ L. S. Levitov, H. Lee, and G. B. Lesovik, *J. Math. Phys.* **37**, 4845 (1996).
 - ⁴ T. Ojanen and T. T. Heikkilä, *Phys. Rev. B* **73**, 020501(R) (2006).
 - ⁵ J. Salo, F. W. J. Hekking, and J. P. Pekola (2006), [cond-mat/0605478].
 - ⁶ V. Brosco, R. Fazio, F. W. J. Hekking, and J. P. Pekola, *Phys. Rev. B* **74**, 024524 (2006).
 - ⁷ T. T. Heikkilä, P. Virtanen, G. Johansson, and F. K. Wilhelm, *Phys. Rev. Lett.* **93**, 247005 (2004).
 - ⁸ J. Ankerhold (2006), [cond-mat/0607020].
 - ⁹ J. Tobiska and Y. V. Nazarov, *Phys. Rev. Lett.* **93**, 106801 (2004).
 - ¹⁰ E. B. Sonin, *Phys. Rev. B* **70**, 140506(R) (2004).
 - ¹¹ J. P. Pekola, *Phys. Rev. Lett.* **93**, 206601 (2004).
 - ¹² J. Ankerhold and H. Grabert, *Phys. Rev. Lett.* **95**, 186601 (2005).
 - ¹³ R. K. Lindell, J. Delahaye, M. A. Sillanpää, T. T. Heikkilä, E. B. Sonin, and P. J. Hakonen, *Phys. Rev. Lett.* **93**, 197002 (2004).
 - ¹⁴ S. Gustavsson, R. Leturcq, B. Simovic, R. Schleser, T. Ihn, P. Studerus, K. Ensslin, D. C. Driscoll, and A. C. Gossard, *Phys. Rev. Lett.* **96**, 076605 (2006).
 - ¹⁵ S. Gustavsson, R. Leturcq, B. Simovic, R. Schleser, P. Studerus, T. Ihn, K. Ensslin, D.C.Driscoll, and A. Gossard (2006), [cond-mat/0605365].
 - ¹⁶ S. Gustavsson, R. Leturcq, T. Ihn, K. Ensslin, M. Reinwald, and W. Wegscheider (2006), [cond-mat/0607192].
 - ¹⁷ A. O. Caldeira and A. J. Leggett, *Ann. Phys.* **149**, 374 (1983).
 - ¹⁸ One could equally well describe voltage fluctuations, but then the spectrum should be calculated for them.
 - ¹⁹ Note that this differs from the one used in Ref. 4 by $4\pi^2$.
 - ²⁰ R. Schoelkopf, A. Clerk, S. Girvin, K. Lehnert, and M. Devoret, *Quantum Noise in Mesoscopic Physics* (Kluwer, Dordrecht, 2003), vol. 97 of *Nato Science Series II*.
 - ²¹ R. Aguado and L. P. Kouwenhoven, *Phys. Rev. Lett.* **84**, 1986 (2000).
 - ²² Note that the Fourier convention in Eq. (3) slightly differs from Eq. (42) in Ref. 5.
 - ²³ Y. Blanter and M. Büttiker, *Phys. Rep.* **336**, 1 (2000).
 - ²⁴ P. Virtanen and T. T. Heikkilä, *New J. Phys.* **8**, 50 (2006).
 - ²⁵ C. W. J. Beenakker, M. Kindermann, and Y. V. Nazarov, *Phys. Rev. Lett.* **90**, 176802 (2003).
 - ²⁶ K. M. Schep and G. E. W. Bauer, *Phys. Rev. Lett.* **78**, 3015 (1997).
 - ²⁷ Y. V. Nazarov, *Phys. Rev. Lett.* **73**, 134 (1994).
 - ²⁸ H. U. Baranger and P. A. Mello, *Phys. Rev. Lett.* **73**, 142 (1994).
 - ²⁹ Here we assume that in the absence of the noise source, the qubit relaxation is independent of the direction of the fields.
 - ³⁰ J. P. Pekola, T. E. Nieminen, M. Meschke, J. M. Kivioja, A. O. Niskanen, and J. J. Vartiainen, *Phys. Rev. Lett.* **95**, 197004 (2005).
 - ³¹ To be precise, we assume here that the inverse mass is perturbed by the current fluctuations. In some cases, the next-order term of the form $(\delta m)^2/m^3$ would also contribute in the third order in $\delta m(\delta I)$.
 - ³² J. B. Majer, F. G. Paauw, A. C. J. ter Haar, C. J. P. M. Harmans, and J. E. Mooij, *Phys. Rev. Lett.* **94**, 090501 (2005).
 - ³³ I. Chiorescu, Y. Nakamura, C. J. P. M. Harmans, and J. E. Mooij, *Science* **299**, 1869 (2003).
 - ³⁴ J. M. Martinis, S. Nam, J. Aumentado, K. M. Lang, and C. Urbina, *Phys. Rev. B* **67**, 094510 (2003).
 - ³⁵ J. M. Martinis, S. Nam, J. Aumentado, and C. Urbina, *Phys. Rev. Lett.* **89**, 117901 (2002).
 - ³⁶ Y. Nakamura, Y. A. Pashkin, and J. S. Tsai, *Nature* **398**, 786 (1999).
 - ³⁷ K. E. Nagaev, S. Pilgram, and M. Büttiker, *Phys. Rev. Lett.* **92**, 176804 (2004).
 - ³⁸ F. W. J. Hekking and J. P. Pekola, *Phys. Rev. Lett.* **96**, 056603 (2006).
 - ³⁹ S. Pilgram, K. E. Nagaev, and M. Büttiker, *Phys. Rev. B* **70**, 045304 (2004).
 - ⁴⁰ Y. Makhlin, G. Schön, and A. Shnirman, *Rev. Mod. Phys.* **73**, 357 (2001).
 - ⁴¹ D. Vion, A. Aassime, A. Cottet, P. Joyez, H. Pothier, C. Urbina, D. Esteve, and M. H. Devoret, *Science* **296**, 886 (2002).
 - ⁴² L. Roschier, M. Sillanpää, and P. Hakonen, *Phys. Rev. B* **71**, 024530 (2005).
 - ⁴³ M. A. Sillanpää, T. Lehtinen, A. Paila, Y. Makhlin, L. Roschier, and P. J. Hakonen, *Phys. Rev. Lett.* **95**, 206806 (2005).
 - ⁴⁴ T. Duty, G. Johansson, K. Bladh, D. Gunnarsson, C. Wilson, and P. Delsing, *Phys. Rev. Lett.* **95**, 206807 (2005).
 - ⁴⁵ The criterion for neglecting the term of the form $(\delta L)^2/(L^2)$ (see Ref. 31) here is $\sin(2\pi\Phi_x/\Phi_0) \gg$

$\cos(2\pi\Phi_x/\Phi_0)$.
⁴⁶ G. B. Lesovik and N. M. Chtchelkatchev, JETP Lett. **77**, 393 (2003).